Electronic Supplementary Information

Facile Strategy to Achieve Vitrimer-Like Elastomer Composites with Lignin as a Renewable Bio-Filler toward Excellent Reinforcement and Recyclability

*Ganggang Zhang[a], Chenchen Tian[b], Heying Chu[c], Jun Liu[*b], Baochun Guo[*a] and Liqun Zhang[*a, b]*

[a]Institute of Emergent Elastomers, School of Materials Science and Engineering, South China University of Technology, Guangzhou, 510640, China

[b]State Key Laboratory of Organic-Inorganic Composites, Beijing University of Chemical Technology, Beijing 100029, P. R. China

[c]College of Mechanical and Electrical Engineering, Tarim University, Alar, Xinjiang, 843300.

*Corresponding authors:

E-mail: zhanglq@mail.buct.edu.cn

E-mail: psbcguo@scut.edu.cn

E-mail: liujun@mail.buct.edu.cn

Number of pages: 9

Number of figures: 8

Number of tables: 7

Characterization.

X-ray spectroscopy (XPS) analysis was performed on a Kratos Axis Ultra DLD equipped with Al Kα radiation source (1486.6 eV). The XPS data were calibrated to the reference graphitic carbon (binding energy of 284.7 eV). A Gaussian sum function and a Shirley background are used for the deconvolution.

Fourier transform infrared (FTIR) spectroscopy was carried out on a Bruker Vertex 70 FTIR spectrometer. Spectra were recorded with wavenumbers ranging from 4000 to 400 cm^{-1} for 32 scans at a resolution of 2 cm^{-1}. Samples were prepared by directly dropping the solution onto KBr films.

The atomic force microscopy (AFM) measurements of the samples were carried out on a Bruker MultiMode AFM equipped with a Nanoscope IV Controller (Veeco Metrology) under ambient conditions.

The tensile properties of the samples were measured using a CMT 4104 tensile instrument (SANS Test Machine Co., Ltd., Shenzhen, China) at ambient temperature. According to the standard ASTM D412, the tensile rate was set to 500 mm/min. Cyclic tensile tests were conducted with a rate of 200 mm/min for both loading and unloading.

Differential scanning calorimetry (DSC) analyses of the samples were conducted using a DSC instrument (Mettler Toledo, Switzerland) with a STARe system under an N_2 atmosphere. The experimental methods are as follows: the samples (5−6 mg) were first heated to 80 °C and held for 5 min to eliminate the thermal history, then cooled down to -60 °C, and finally heated again to 40 °C with a heating rate of 10 °C/min. The values of glass transition temperature (Tg) were obtained from the second heating cycle by the half-delta Cp method.

The dynamic mechanical analyses (DMTA) of the samples were conducted using a NETZSCH DMA 242 device (Netzsch-Gerätebau GmbH, Germany) under a tension mode. The strain amplitude and a frequency were set to 0.3% and 10 Hz, respectively. The testing temperature was set from −80 to 80 °C, and the heating rate was set to 3 K/min.

Stress relaxation and creep experiments were carried out on a DMA Q800 analyzer (TA Instruments, USA). For the stress relaxation test, the samples were first preloaded by a force of 1×10^{-3} N and were stretched to a constant strain of 1% over time after equilibrating for 5 min at desired temperatures. The characteristic relaxation time (τ^*) could be defined as the time required to relax to $1/e$ of initial stress.

Thermal gravimetric analysis (TGA) was performed on a TA Q50 thermogravimetric analyzer under an air atmosphere at a heating rate of 10 °C/min.

Equilibrium swelling experiments. The vulcanizates were immersed in toluene at room temperature for 72 h. Subsequently, the samples are removed from the solvent and immediately weighed after wiping off the surface toluene. The samples were further dried in a vacuum oven at 60 °C until constant weight. The sol fraction is calculated according to $(m_0\text{-}m_2)/m_0$, and the swelling ratio is defined as $(m_1\text{-}m_2)/m_2$, where m_0 is the weight of the sample before swelling; m_1 and m_2 are the sample weights before and after drying, respectively. The crosslinking density was determined as the classical Flory-Rehner equation.

$$V_e = \frac{\ln\left(1 - V_r\right) + V_r + \chi {V_r}^2}{V_s({V_r}^{1/3} - V_r/2)}$$

where V_r is the volume fraction of elastomer in the swollen gel, V_s is the molar volume of the solvent (106.5 cm^3/mol for toluene), and χ is the Flory-Huggins solvent-polymer interaction parameter ($\chi_{SBR\text{-}toluene}$ is 0.0653). V_r was calculated according to the following equation:

$$V_r = \frac{(m_2 - m_0\varphi)/\rho_r}{(m_2 - m_0\varphi)/\rho_r + (m_1 - m_2)/\rho_s}$$

where φ is the weight fraction of the insoluble components, and ρ_r and ρ_s are the density of elastomer and solvent, respectively.

To monitor the photothermal temperature changes of lignin/VPR composite, NIR laser with adjustable output power (λ = 808 nm, Ningbo Yuanming Laser Technology Co., Ltd., China) was used as the light source. To monitor the temperature change, thermal infrared images were recorded using a FLIR E30 infrared camera (FLIR Systems, Inc., USA). The power density ($W \cdot cm^{-2}$) refers to the light intensity irradiated on the sample per unit area (cm^{-2}), which was adjusted by the distance between the light source and sample and was tested by an optical power meter.

Table S1. The raw material formulas for the lignin/VPR compounds.

Samples	VPR content (g)	Lignin content (g)	$ZnCl_2$ content (g)	DIH content (g)
L0Zn0	100	0	0	6
L0Zn6	100	0	6	6
L60Zn6	100	60	6	6
L60Zn0	100	60	0	6
L60Zn2	100	60	2	6
L60Zn4	100	60	4	6
L40Zn4	100	40	6	6
L50Zn5	100	50	5	6
L70Zn7	100	70	7	6

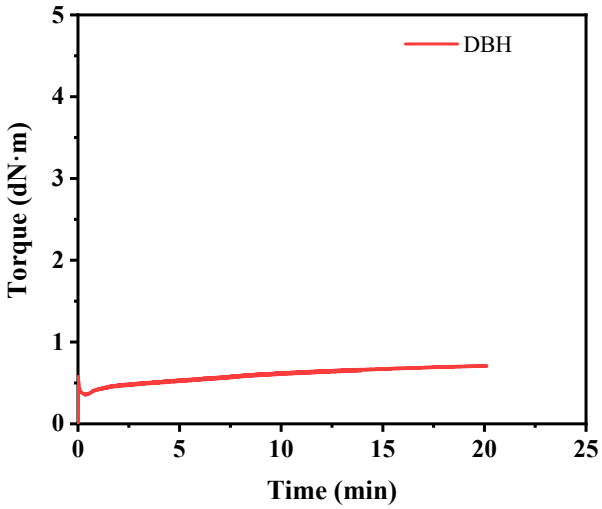

Figure S1. Curing curves at 180 °C of the lignin/VPR composites with 1,6-dibromhexane (DBH) as a cross-linker

Table S2. The curing characteristic parameters of VPR compounds with DIH as a crosslinker

Samples	M_L (dN·m)	M_H (dN·m)	△M(M_H-M_L) (dN·m)	t_{10} (min)	t_{90} (min)
L0Zn0	0.3	1.7	1.4	1.7	37.9
L0Zn6	0.3	4.2	3.9	2.5	44.2
L60Zn6	0.9	6.5	5.6	16.5	44.0

Table S3. Mechanical property parameters of VPR vulcanizates with DIH as a crosslinker

Samples	Tensile strength (MPa)	Modulus at 100% (MPa)	Modulus at 300% (MPa)	Elongation at break (%)	Shore A hardness
L0Zn0	2.4±0.2	0.7±0	2.1±0.1	331±21	
L0Zn6	5.9±1.1	2.4±0.3		233±38	
L60Zn6	12.4±0.2	8.5±0.2	-	211±11	77

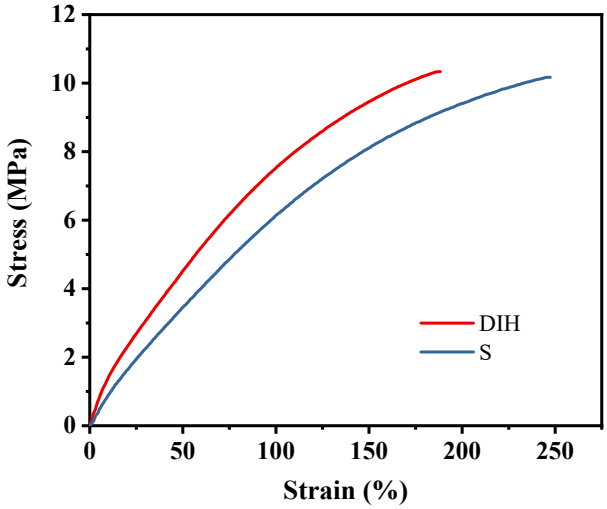

Figure S2. Typical stress-strain curves of the lignin/VPR composites based on different curing systems.

Table S4. The curing characteristic parameters of VPR compounds with various lignin content

$ZnCl_2$ content (phr)	M_L (dN·m)	M_H (dN·m)	△M(M_H-M_L) (dN·m)	t_{10} (min)	t_{90} (min)
0	0.5	3.6	3.1	1.7	19.4
2	0.7	5.1	4.4	2.9	25.0
4	0.8	6.0	5.2	3.7	36.1
6	0.9	6.5	5.6	16.5	44.0

Table S5. Mechanical property parameters of the lignin/VPR composites with various $ZnCl_2$ content

$ZnCl_2$ content (phr)	Tensile strength (MPa)	Modulus at 100% (MPa)	Elongation at break (%)	Shore A hardness
0	6.1±0	4.0±0.1	215±9	60
2	8.5±0.1	6.0±0.2	187±10	68
4	10.3±0.3	7.5±0.2	188±6	73
6	12.4±0.2	8.5±0.2	211±11	77

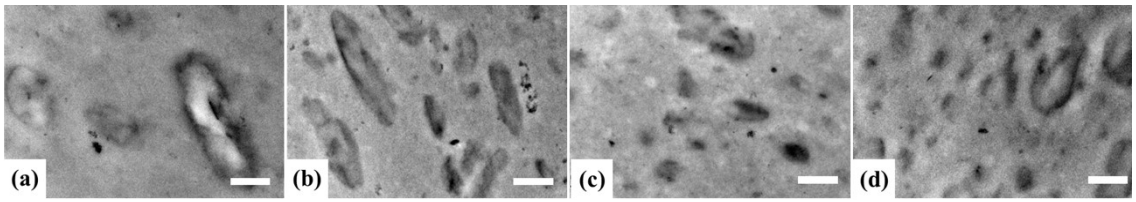

Figure S3. TEM images of lignin/VPR composites with various $ZnCl_2$ content (phr): (a) 0, (b) 2, (c) 4, (d) 6. (scale bar, 200 nm)

Table S6. The curing characteristic parameters of VPR compounds with various lignin content

Lignin content (phr)	M_L (dN·m)	M_H (dN·m)	△M(M_H-M_L) (dN·m)	t_{10} (min)	t_{90} (min)
40	0.5	5.4	4.9	13.4	35.9
50	0.8	5.8	5.0	16.4	43.8
60	0.9	6.5	5.6	16.5	44.0
70	1.0	6.8	5.8	18.9	49.3

Table S7. Mechanical property parameters of the lignin/VPR composites with various lignin content

lignin content (phr)	Tensile strength (MPa)	Modulus at 100% (MPa)	Elongation at break (%)	Shore A hardness
40	10.5±0.4	5.2±0.1	282±21	68
50	11.9±0.3	7.3±0.1	252±18	73
60	12.4±0.2	8.5±0.2	211±11	77
70	14.1±0.2	11.2±0.1	188±11	82

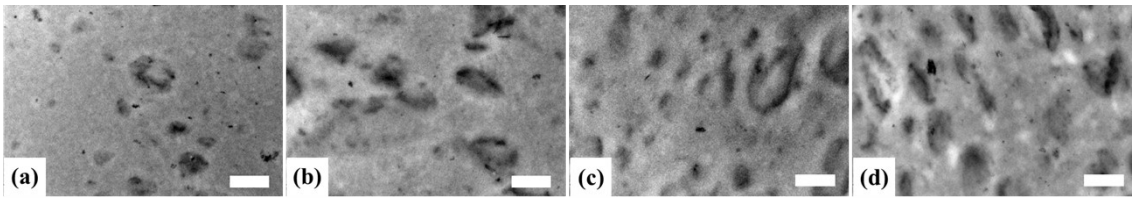

Figure S4. TEM images of lignin/VPR composites with various lignin content (phr): (a) 40, (b) 50, (c) 60, (d) 70. (scale bar, 200 nm)

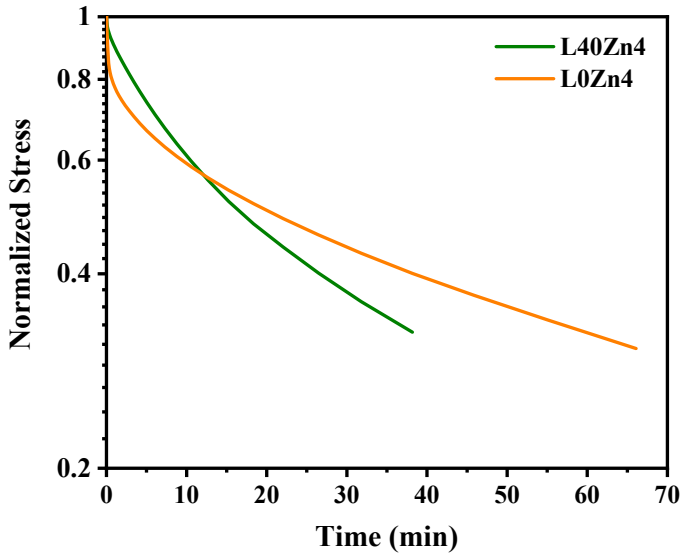

Figure S5. Normalized stress relaxation for the L40Zn4 and L0Zn4 sample at 190 °C

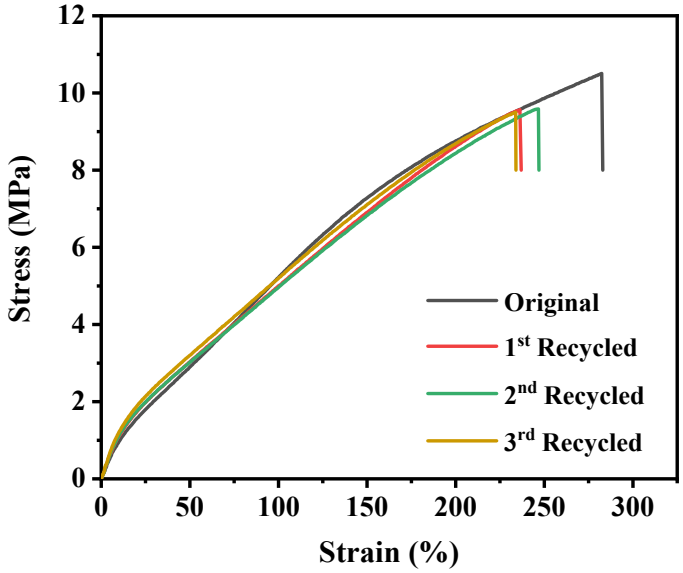

Figure S6. Typical stress−strain curves of the L40Zn4 sample after multiple reprocessing cycles

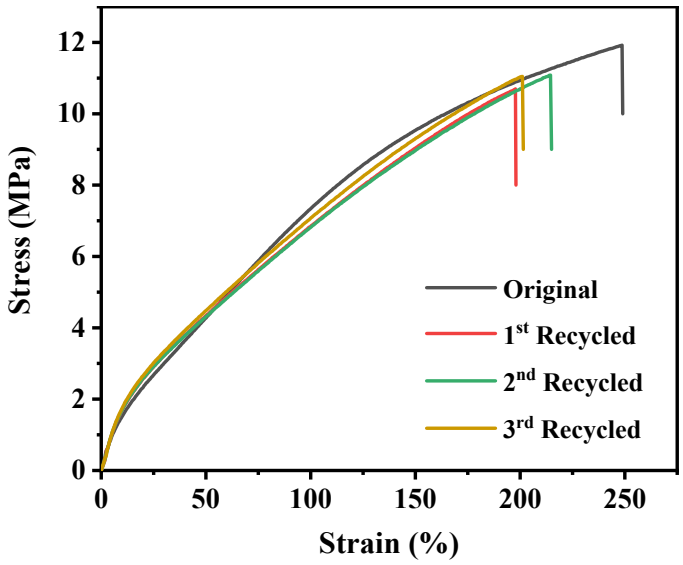

Figure S7. Typical stress−strain curves of the L50Zn5 sample after multiple reprocessing cycles

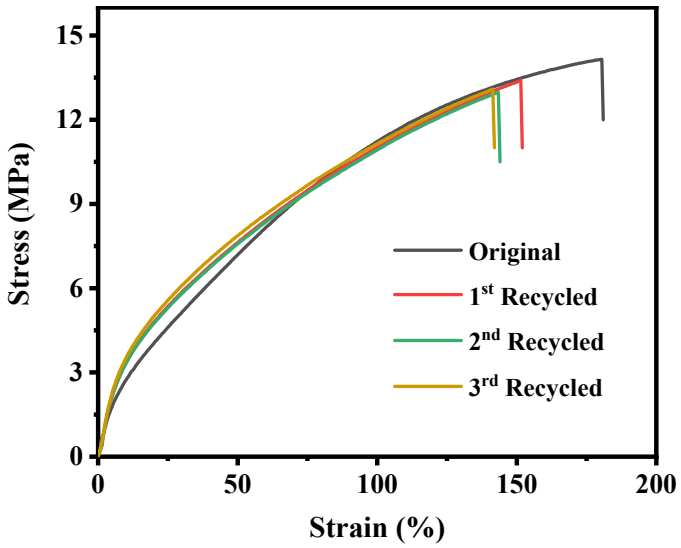

Figure S8. Typical stress−strain curves of the L70Zn7 sample after multiple reprocessing cycles

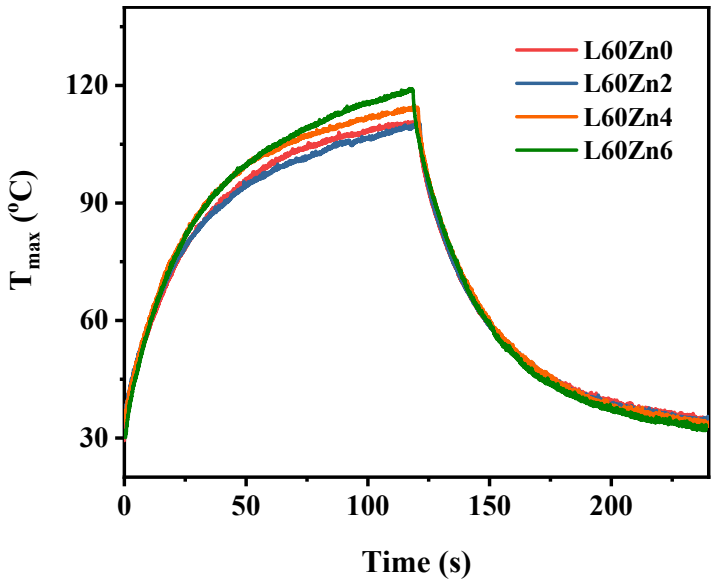

Figure S9. Changes in the surface temperature of the samples with various $ZnCl_2$ content